BIOCHEMISTRY
including biophysical chemistry & molecular biology

Rapid Report

pubs.acs.org/biochemistry

Site-Specific Fluorescence Dynamics of α-Synuclein Fibrils Using Time-Resolved Fluorescence Studies: Effect of Familial Parkinson's Disease-Associated Mutations

Shruti Sahay,[†] A. Anoop,[†] G. Krishnamoorthy,*[,‡] and Samir K. Maji*[,†]

[†]Department of Biosciences and Bioengineering, IIT Bombay, Powai, Mumbai 400076, India

[‡]Department of Chemical Sciences, Tata Institute of Fundamental Research, Mumbai 400005, India

Supporting Information

ABSTRACT: α-Synuclein (α-Syn) aggregation is directly implicated in both the initiation and spreading of Parkinson's Diseases (PD) pathogenesis. Although the familial PD-associated mutations (A53T, E46K, and A30P) are known to affect the aggregation kinetics of α-Syn *in vitro*, their structural differences in resultant fibrils are largely unknown. In this report we studied the site-specific dynamics of wild type (wt) α-Syn and its three PD mutant fibrils using time-resolved fluorescence intensity, anisotropy decay kinetics, and fluorescence quenching. Our data suggest that the N- and C-terminus are more flexible and exposed compared to the middle non-amyloid-β component (NAC) region of wt and PD mutant α-Syn fibrils. Yet the N-terminus showed great conformational heterogeneity compared to the C-terminus for all these proteins. 71 position of E46K showed more flexibility and solvent exposure compared to other α-Syns, whereas both E46K and A53T fibrils possess a more rigid C-terminus compared to wt and A30P. The present data suggest that wt and PD mutant fibrils possess large differences in flexibility and solvent exposure at different positions, which may contribute to their different pathogenicity in PD.

The 140-residue protein α-Synuclein (α-Syn) has been linked to Parkinson's disease (PD), a common neurodegenerative disease pathologically characterized by the presence of intraneuronal inclusions (Lewy bodies) mainly composed of fibrillar aggregates of α-Syn.[1] Several genetic, animal models of PD and cell culture studies suggest that aggregation of α-Syn into amyloid fibrils is the major pathogenic event in PD.[2,3] Moreover missense mutations (A53T, E46K, A30P and newly discovered H50Q, G51D) duplication and triplication of the locus of the α-Syn gene associated with rare familial forms of the disease implicate the central role of α-Syn in PD pathogenesis.[4] Overexpression of wt α-Syn and its PD-associated mutants in cultured neurons and various transgenic animal models recapitulate several characteristics of PD.[3] The effect of familial PD-associated mutations (A53T, E46K, A30P) on the *in vitro* aggregation kinetics of α-Syn has been widely studied.[3] Yet their effect on the fibril structure and dynamics of α-Syn is not well-known. Although many studies have suggested that α-Syn oligomers are highly cytotoxic,[5,6] reports of α-Syn fibrils being cytotoxic having the ability to bind and damage the plasma membrane in cells are also present.[7] It has not yet been clearly established which entity is the most potent neurotoxic species contributing to PD pathogenesis. Recent studies have suggested α-Syn fibrils are infectious and exogenously added α-Syn fibrils could be internalized and template the fibril formation of endogenous α-Syn in the cells.[8] Interestingly, it has been shown that α-Syn forms polymorphic fibrils with different structural and functional behavior.[9] Thus, in light of the current scenario it is quite intriguing to study the effect of PD-associated mutations on the structure and dynamics of α-Syn fibrils, which could also lead to their different pathogenic properties. The effect of PD-associated mutations on the monomeric structure of α-Syn was studied recently using various biophysical methods including NMR and molecular dynamics (MD) simulations, which showed that wild-type (wt), E46K, A53T, and A30P α-Syns have different long-range intramolecular interactions.[10−13] Previous biophysical studies have provided insight into the overall structural organization of α-Syn fibrils, which suggest that the middle region comprising the residues ∼35−100 forms the β-sheet rich fibril core, whereas the N- and C-terminal segments remain unprotected and flexible in α-Syn fibrils.[14−16] It is known that the middle non-amyloid-β component (NAC) region of α-Syn is responsible for its fibrillizing ability and the C-terminal domain regulates its fibrillation, whereas the N-terminus binds to lipids [3] (Supporting Information (SI)).

Although there are a few recent reports on the effect of PD-associated mutations (E46K, A53T, and A30P) on α-Syn fibril structure,[17] how the familial disease associated mutations affect the domain specific structure of α-Syn fibrils is not yet known. Therefore, we used time-resolved fluorescence to study the site-specific dynamics and structural readouts of different regions (N-terminal, C-terminal, and middle NAC region) of α-Syn and its familial mutants in the fibrillar form. Tryptophan (Trp) residue was substituted at specific sites in each of the three regions of wt α-Syn and its PD mutants (Figure 1A, Table S1) using site-directed mutagenesis. Since [V^3W]E46K protein had a much lower expression level and protein yield, we designed another Trp mutant [F^4W] at the N-terminus of E46K for our study (Figure 1A). Protein expression, purification, and low-molecular weight (LMW) preparation was done using

Received: November 16, 2013
Revised: January 22, 2014
Published: January 22, 2014

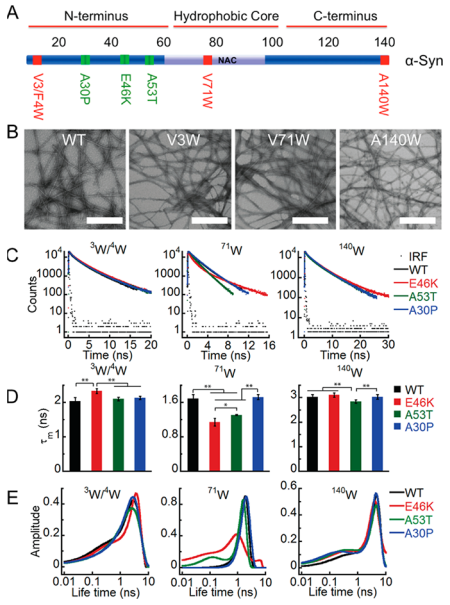

Figure 1. (A) Schematic representation of different regions of α-Syn sequence, the three PD-associated mutations, and the three Trp mutations designed for the study. (B) EM images of fibrils formed by wt α-Syn and its three designed Trp mutants. Scale bar represents 500 nm. Site-specific microenvironment studied using time-resolved fluorescence intensity decay kinetics. (C) Discrete analysis of intensity decays using a three exponential function. (D) Mean lifetime ($\tau_m = \Sigma\alpha_i \tau_i$) values derived from discrete analysis represented as bar diagram (mean ± s.d., $n = 3$). (E) Fluorescence lifetime distributions obtained from Maximum Entropy Method (MEM) analysis of intensity decays for $^3W/^4W$, ^{71}W, and ^{140}W of wt as well as PD mutant α-Syn fibrils.

previously published protocols[5,18] (SI). The LMW form of all proteins in [20 mM Gly-NaOH (pH 7.4) and 0.01% sodium azide] at 300 μM concentration were allowed to fibrillize by incubating them at 37 °C with slight agitation (SI). After 10 days of incubation, all the proteins formed amyloid fibrils as observed by electron microscopy (EM) (Figures 1B and S2). No significant difference in the fibril morphology was observed by EM of wt, A53T, E46K, and A30P α-Syn as well as the Trp mutated proteins (Figure S2). The secondary structural transition was analyzed for all proteins by circular dichroism (CD), which shows random coil at the beginning (LMW form) to β-sheet transition on aggregation into fibrils (after incubation) (Figure S1). Fibrils were isolated from the incubated solutions by centrifugation (SI). We studied different aspects of site-specific dynamics of the fibrils; the microenvironment experienced by the probe was studied using time-resolved fluorescence intensity decay kinetics and steady-state fluorescence, conformational flexibility was studied using time-resolved anisotropy decay kinetics, and the solvent exposure was studied using acrylamide quenching of fluorescence (details are described in SI).

Steady-state Trp fluorescence spectra suggest that the N- ($^3W/^4W$) and C-terminus (^{140}W) experience relatively polar microenvironments as their emission maxima (λ_{max}) are ~350 nm for all proteins, whereas ^{71}W of the middle region (λ_{max} 317 nm for wt, A53T, and A30P; 330 nm for E46K) is buried in the core of the fibrils for all α-Syns (Figure S3A). Site-specific microenvironments for all proteins were further studied by time-resolved fluorescence intensity decay kinetics, which shows strikingly different environments for wt and PD mutant fibrils at the ^{71}W position (Figure 1C). All the decay kinetics were fitted to a three exponential function (SI Table S3). The mean lifetime ($\tau_m = \Sigma\alpha_i \tau_i$) values derived from the discrete analysis of the intensity decays show differences at all three different positions of wt and PD mutants of α-Syn. The ^4W in E46K fibrils has a higher τ_m than that of ^3W in the other three α-Syn (wt, A53T, and A30P) fibrils (Figure 1D). The ^{140}W in A53T fibrils has a lower τ_m than that of the other three α-Syn fibrils (Figure 1D). The τ_m of ^{71}W in E46K and A53T fibrils as compared to wt and A30P fibrils is significantly small (Figure 1D). This shows that the structure and dynamics of the fibrils, especially at the core region, are modulated in the mutants, E46K and A53T. Fluorescence intensity decays were further analyzed by the maximum entropy method (MEM) to delineate structural heterogeneity.[19] Lifetime distributions derived from MEM analysis show dual peaks at the N- and C-terminal Trp of all fibrils and 71 position (NAC region) of E46K and A53T mutant fibrils (Figure 1E). The data indicate structural heterogeneity in these sites of different α-Syns. Also the N-terminus ($^3W/^4W$) experiences an even more heterogeneous local environment as reflected by its broad lifetime distributions compared to the middle (^{71}W) and C-terminus (^{140}W) for all α-Syn fibrils (Figure 1E). Similarly, the ^{71}W in E46K fibrils has relatively broadened lifetime distributions indicating its increased conformational heterogeneity as compared to that in wt, A30P, and A53T α-Syn fibrils (Figure 1E). Interestingly, the major peak in the lifetime distributions shifts to shorter lifetime values at the 71 position only (Figure 1E) further indicating that the NAC region experiences a different site-specific microenvironment compared to the N- and C-terminus in all α-Syn fibrils.

Further, the site-specific conformational flexibility of the fibrils was studied using time-resolved fluorescence anisotropy decay kinetics. Anisotropy decays of all fibrils were fitted satisfactorily to a sum of two exponentials, a model assuming a population having uniform fluorescence dynamics properties with each fibril associated with two rotational correlation times (Figure 2A, SI Table S4). The two rotational correlation times were interpreted to be associated with the local motion of Trp (shorter correlation time, ϕ_1) and the global motion (longer

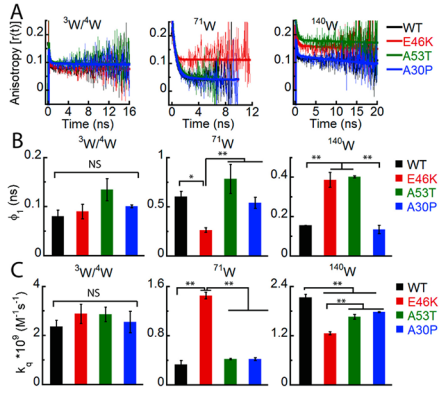

Figure 2. (A) Time-resolved anisotropy decay kinetics fitted to a two exponential function; smooth lines are fits to eqs 4–6 (SI). (B) Rotational correlation time associated with the local motion of Trp (ϕ_1) derived from the fitting of anisotropy decay; represented as bar diagram (mean ± s.d., $n = 2$). (C) Differential solvent exposure measured by bimolecular quenching rate constant (k_q) values derived from the Stern–Volmer plots; represented as bar diagram (mean ± s.d., $n = 3$) for $^3W/^4W$, ^{71}W, and ^{140}W of wt as well as PD mutant α-Syn fibrils.

dx.doi.org/10.1021/bi401543z | Biochemistry 2014, 53, 807–809

correlation time, ϕ_2) of the entire fibril. Therefore the shorter rotational correlation time (ϕ_1) would give an idea of the site-specific dynamics of fibrils. At the N-terminus (^{3}W/^{4}W), the fibrils of all α-Syns have very similar dynamics (ϕ_1 values are almost the same for wt and PD mutant fibrils) (Figure 2A, B). However, the PD mutations have an effect at the middle and C-terminus. At ^{71}W, E46K fibrils have a shorter ϕ_1 as compared to that in wt, A30P, and A53T fibrils, indicating ^{71}W is in a more dynamic environment in E46K fibrils (Figure 2A, B). Moreover at the 140 position, ϕ_1 is larger for E46K and A53T fibrils as compared to wt and A30P fibrils, which suggests that ^{140}W is more rigid in E46K and A53T fibrils (Figure 2A, B).

Finally, the site-specific solvent exposures at three different positions were studied by acrylamide quenching of Trp fluorescence. The extent of solvent exposure was estimated by calculating k_q (bimolecular quenching rate constant) using the slope of Stern−Volmer plots (Figure S3B) and τ_m values (SI). The results show that the N- (^{3}W/^{4}W) and C-terminus (^{140}W) are relatively more solvent-exposed as compared to the middle (^{71}W) in all α-Syn fibrils consistent with the steady-state fluorescence results (Figures 2C, S3A). ^{3}W/^{4}W has no significant difference in solvent exposure when compared for wt and PD mutant fibrils (Figure 2C). However at the 140 position, all the PD mutant fibrils show reduced solvent exposure compared to the wt indicating the buried nature of ^{140}W (Figure 2C). Also at the 71 position, E46K fibrils are relatively more solvent-exposed as compared to other α-Syn fibrils (Figure 2C) (for detailed analysis see SI).

Overall our data suggest that, for wt α-Syn and its PD-associated mutants, the N- (^{3}W/^{4}W) and C-terminus (^{140}W) are conformationaly flexible and solvent-exposed whereas the middle region (^{71}W) is conformationaly rigid and buried inside the core of fibrils. This is in agreement with the existing data on α-Syn fibril structure.[14−16] Moreover the N-terminus exhibits great structural heterogeneity in all α-Syn fibrils. Additionally our results show that the fibrils formed by wt and PD-associated mutant α-Syns have significant site-specific differences in structure and dynamics. Strikingly, the C-terminus (^{140}W), despite not being a part of the fibril core, possesses some conformational restrictions, which are affected by the PD-associated mutations. A30P and wt α-Syn fibrils are more conformationaly flexible at the 140 position as compared to E46K and A53T fibrils. Interestingly, E46K and A53T fibrils have a markedly altered and heterogeneous environment at the middle (71 position) as compared to wt and A30P α-Syn fibrils, consistent with the previous reports.[17] Furthermore, our results suggest that the mutation of E46K results in a more flexible and solvent exposed core (71 position) of α-Syn fibrils. The tertiary structural differences for the E46K mutant in the monomeric form were already reported by Wise-Scira et al.,[12] and this study shows an enhancement and proves it to be true for the fibrils as well. Moreover, alterations in structure and dynamics caused by the PD mutations at locations far from their site (such as observed at position 140) is most unexpected and warrant further study. The faster fibrillizing mutants A53T and E46K cause the major alterations in the structure and dynamics at the C-terminus and middle region of fibrils. It is possible that the A53T and E46K mutations that lie in the β-sheet rich region of the fibril core (residues ∼38−95)[14,15,17] might perturb the β-sheet arrangement of the core to a greater extent compared to A30P mutation, which lies at the extreme end of the core structure. However it is not clear at this point whether the observed differences in site-specific structure and dynamics of the fibrils of wt α-Syn and its disease associated mutants contribute to their pathology in PD (discussion provided in SI). Nevertheless the present study expands our understanding of the structure and dynamics of the fibrils of wt α-Syn and its PD-associated mutants. This may also contribute to establishing the structure−phenotypic relationship of these proteins in PD pathogenesis.

■ ASSOCIATED CONTENT

Supporting Information

Description of material methods, figures, and tables. This material is available free of charge via the Internet at http://pubs.acs.org.

■ AUTHOR INFORMATION

Corresponding Authors

*E-mail: gk@tifr.res.in. Phone: 91-22-2278 2301.

*E-mail: samirmaji@iitb.ac.in. Phone: 91-22-2576 7774.

Funding

The work was supported DBT grants (BT/PR14344Med/30/501/2010; BT/PR13359/BRB/10/752/2009).

Notes

The authors declare no competing financial interest.

■ ACKNOWLEDGMENTS

Authors acknowledge Central EM Facility (IRCC, IIT Bombay). S.S. is thankful to Shyama Prasad Mukherjee Fellowship (CSIR). G.K. is a recipient of the J.C. Bose Fellowship of the Govt. of India.

■ REFERENCES

(1) Spillantini, M. G., Crowther, R. A., Jakes, R., Hasegawa, M., and Goedert, M. (1998) *Proc. Natl. Acad. Sci. U.S.A. 95*, 6469.

(2) Lansbury, P. T., Jr., and Brice, A. (2002) *Curr. Opin. Genet. Dev. 12*, 299.

(3) Deleersnijder, A., Gerard, M., Debyser, Z., and Baekelandt, V. (2013) *Trends Mol. Med. 19*, 368.

(4) Fujioka, S., Ogaki, K., Tacik, P. M., Uitti, R. J., Ross, O. A., and Wszolek, Z. K. (2014) *Parkinsonism Relat. Disord. 20* (Suppl 1), S29.

(5) Winner, B., et al. (2011) *Proc. Natl. Acad. Sci. U.S.A. 108*, 4194.

(6) Karpinar, D. P., et al. (2009) *EMBO J. 28*, 3256.

(7) Pieri, L., Madiona, K., Bousset, L., and Melki, R. (2012) *Biophys. J. 102*, 2894.

(8) Luk, K. C., et al. (2009) *Proc. Natl. Acad. Sci. U.S.A. 106*, 20051.

(9) Bousset, L., et al. (2013) *Nat. Commun. 4*, 1.

(10) Coskuner, O., and Wise-Scira, O. (2013) *ACS Chem. Neurosci. 4*, 1101.

(11) Wise-Scira, O., Aloglu, A. K., Dunn, A., Sakallioglu, I. T., and Coskuner, O. (2013) *ACS Chem. Neurosci. 4*, 486.

(12) Wise-Scira, O., Dunn, A., Aloglu, A. K., Sakallioglu, I. T., and Coskuner, O. (2013) *ACS Chem. Neurosci. 4*, 498.

(13) Bertoncini, C. W., Fernandez, C. O., Griesinger, C., Jovin, T. M., and Zweckstetter, M. (2005) *J. Biol. Chem. 280*, 30649.

(14) Vilar, M., et al. (2008) *Proc. Natl. Acad. Sci. U.S.A. 105*, 8637.

(15) Heise, H., Hoyer, W., Becker, S., Andronesi, O. C., Riedel, D., and Baldus, M. (2005) *Proc. Natl. Acad. Sci. U.S.A. 102*, 15871.

(16) Chen, M., Margittai, M., Chen, J., and Langen, R. (2007) *J. Biol. Chem. 282*, 24970.

(17) Comellas, G., et al. (2011) *J. Mol. Biol. 411*, 881.

(18) Singh, P. K., Kotia, V., Ghosh, D., Mohite, G. M., Kumar, A., and Maji, S. K. (2013) *ACS Chem. Neurosci. 4*, 393.

(19) Lakshmikanth, G. S., Sridevi, K., Krishnamoorthy, G., and Udgaonkar, J. B. (2001) *Nat. Struct. Biol. 8*, 799.